1 Title: Extraction-free direct PCR from dried serum spots permits HBV genotyping and RAS

2 identification by Sanger and minION sequencing

3 Running title: Sequencing of hepatitis B virus directly from dried serum spot

4 Stuart Astbury[a,b,c], Marcia Maria Da Costa Nunes Soares[d], Emmanuel Peprah[e], Barnabas

5 King[b,e], Ana Carolina Gomes Jardim[f], Jacqueline Farinha Shimizu[f], Paywast Jalal[g], Chiman H

6 Saeed[h], Furat T Sabeer[i], William L Irving[b,c,e], Alexander W Tarr[b,c,e*], C Patrick McClure[b,e]

7

8 [a] Nottingham Digestive Diseases Centre, School of Medicine, University of Nottingham, UK

9 [b] NIHR Nottingham Biomedical Research Centre, Nottingham University Hospitals NHS Trust

10 and the University of Nottingham, UK

11 [c] MRC/EPSRC Nottingham Molecular Pathology Node, University of Nottingham, UK

12 [d] Instituto Adolfo Lutz, Brazilian Ministry of Health, São Paulo, Brazil

13 [e] School of Life Sciences, University of Nottingham, UK

14 [f] Institute of Biomedical Sciences, Federal University of Uberlândia, Uberlândia, Brazil.

15 [g] Biology Department, Faculty of Science, University of Sulaimani, Sulaymaniyah, Iraq

16 [h] Medical Research Center, Hawler Medical University, Erbil, Iraq

17 [i] Central Public Health Laboratory, Erbil, Iraq

18 *Corresponding author: alex.tarr@nottingham.ac.uk

19 **Word count (3,000 limit; excluding abstract, Methods, References, Tables and Figure**

20 **Legends): 2967**

Abstract

In order to achieve the commitment made by the World Health Organisation to eliminate viral hepatitis by 2030, it is essential that clinicians can obtain basic sequencing data for hepatitis B virus (HBV) infected patients. While accurate diagnosis of HBV is achievable in most clinical settings, genotyping and identification of resistance-associated substitutions (RAS) present a practical challenge in regions with limited healthcare and biotechnology infrastructure. Here we outline two workflows for generating clinically relevant HBV sequence data directly from dried serum spot (DSS) cards without DNA extraction using either Sanger, or the portable MinION sequencing platforms. Data obtained from the two platforms were highly consistent and allowed determination of HBV genotype and RAS. This is the first demonstration of MinION sequencing from DSS, illustrating the broad utility of this sequencing technology. We demonstrated the clinical application of this technology using sera sampled on DSS cards obtained from both Iraq and Brazil. The sample stability provided by DSS cards, combined with the rapid PCR and sequencing protocols will enable regional/national centres to provide information relevant to patient management. By providing viable workflows for both the Sanger and MinION sequencing platforms, which vary greatly in the infrastructure and expertise required, we demonstrate that MinION sequencing is a viable method for HBV genotyping in resource-limited settings. These workflows could also be applied to sequencing of other blood borne DNA viruses and bacterial pathogens.

Abstract word count: 230

Introduction

Hepatitis B virus (HBV) infects 257 million people worldwide and causes 887,000 deaths per year, many due to hepatocellular carcinoma (HCC) (1). A recent editorial in *Nature* described HBV as neglected, particularly in Sub-Saharan Africa, where around 6% of the population are infected and only one-tenth of children are vaccinated (2). There is an urgent need for screening and surveillance tools to assess HBV in low and middle-income countries (3). HBV displays a higher degree of diversity relative to other DNA viruses due to a complex and error prone replication cycle involving RNA intermediates, as such it has a mutation rate of around 1.4-3.2 x 10^{-5} mutations/site/year (4). There are many well-characterised mutations across the HBV genome, conferring resistance to therapy or an increase in replication efficiency (polymerase), immune and diagnostic test escape (S/pre-core), or an increase in tumorigenesis (reviewed in (5)).

Next generation sequencing (NGS) enables the study of a population of viral genomes within a single patient, as opposed to Sanger sequencing, which will theoretically provide a "consensus" sequence of the most abundant template. NGS platforms such as those established by Illumina rely on the use of short reads (max 250bp) which are assembled to from a contiguous sequence. Third generation sequencing platforms such as the Oxford Nanopore (ONT) MinION enable sequencing with theoretically no upper limit on read length, meaning entire viral genes or genomes can be sequenced in a single read. The MinION sequencer is also extremely portable and can be powered through a laptop, removing the need for a continuous power supply and enabling sequencing in locations without access to conventional lab facilities. The portable aspect of MinION sequencing has already been demonstrated to great effect during the Ebola outbreak in West Africa (6), and in tracking the spread of Zika virus in Brazil (7). Field application of the MinION platform has

been enhanced with recent advances including improved “R9.4” flow cells with increased accuracy and software such as Nanopolish (8), which works with signal-level data from the sequencer allowing generation of more accurate consensus sequences. However, despite the emerging potential of NGS technologies, Sanger sequencing remains the gold standard in clinical applications and represents the most accessible and affordable choice globally.

We thus aimed to combine both Sanger and MinION sequencing with dried serum spot (DSS) sampling, to develop a method by which HBV can be rapidly sequenced for both genotype as well as potential resistance-associated substitutions (RAS) that can be applied in regions without access to conventional sample storage or a cold chain. As this assay targets the overlapping ORFs containing S and the reverse transcriptase domain of the polymerase gene it can be used to genotype and detect resistance to antiretroviral treatment. HBV genomes are particularly well suited to direct PCR, enabling a clinical sample to be added directly to a PCR reaction with no extraction steps. However, with minor alterations this method can be applied to a wide range of viruses or bacterial pathogens.

Methods

Samples: Thirty HBV DNA-positive serum samples, with known viral load, were obtained from eight specialized centres in São Paulo State, Brazil, collected between July 2016 and April 2017. Samples varied in virus titre from 6.35 x10^2 to 8.16 x 10^8 international units (IU)/mL. In addition, 70 serum samples identified as HBV DNA-positive were collected and processed at the Erbil Central Laboratory, Iraq, in 2017. Samples varied in virus titre from 22 to 9.4 x 10^8 IU/mL. The initial cohort of samples for sequence determination and primer optimisation were obtained from Nottingham University Hospitals NHS Trust, Nottingham, UK, and were held under ethical approval of the Nottingham Health Science Biobank. All samples were obtained for routine diagnostic investigation and surplus material was used in this study. Serum was stored at -70 °C prior to direct use or spotting in Nottingham and -20 °C in Brazil and Iraq.

Viral load determination: Viral load in the Brazilian samples was determined by RealTime HBV Amplification Kit (Abbott). In Iraq, DNA was extracted from 200µl serum using the EZ1 Virus Mini Kit v2.0 (Qiagen), and viral load determined by Artus HBV PCR kit (Qiagen).

Preparation of dried serum spot (DSS) cards: A volume of 25-30 µL serum was spotted onto a Whatman® Protein Saver™ 903 Card (GE Healthcare), air-dried at room temperature for approximately 2 hours and stored at 4 °C until further use. 25 µL of serum typically saturated the 113.1 mm^2 (12 mm diameter) area demarcated on the DSS cards, thus a 3mm diameter punch (7.07 mm^2 area) represented approximately 1.5 µL of serum. Between each sample a clean 3mm^2 punch was made to prevent sample carryover, and a clean filter paper control was included in each PCR run.

PCR: HBV S gene-specific primers of HBV are shown in table 1. Two different modified polymerase enzymes were evaluated for this method: Hemo KlenTaq (NEB) and Phusion

112 Blood Direct (Thermo Fisher). Hemo KlenTaq reactions were set up as 25 µL reactions
113 containing 5 µL Hemo KlenTaq reaction buffer, 0.2 mM dNTP (Sigma), 2 µL Hemo KlenTaq
114 enzyme, 0.3 µM of each primer and 2 µL serum. Phusion Blood Direct reactions were also
115 set up as 25µL reactions containing 12.5 µL 2x Phusion Blood Direct mastermix, 0.5 µM of
116 each primer, 8.5 µL water and 2µL of serum. DSS reactions were prepared in the same way,
117 with a 3 mm^2 punch used in place of serum and the volume adjusted to 25 µL with water.
118 Cycling conditions were as follows, for Phusion Blood Direct: 98 °C for 5 minutes, 55 cycles
119 of [98 °C for 1 second, 50 °C for 5 seconds and 72 °C for 20 seconds/kb], and a final
120 extension at 72 °C for 1 minute. Cycling conditions for Hemo KlenTaq were: 95 °C for 3
121 minutes, 55 cycles of [95 °C for 20 seconds, 50 °C for 30 seconds and 68 °C for 2
122 minutes/kb], and a final extension at 68 °C for 10 minutes. The sensitivity of this assay with
123 different primer pairs was also tested by serially diluting a high viral titre sample (1.2×10^7
124 IU/mL) logarithmically down to 1.2×10^1 IU/mL.

125 Initially a well cited primer set (F1 and R1) generating a short amplicon in a conserved
126 genomic sequence towards the end of the S gene (9) was used to probe the maximum
127 sensitivity of direct PCR from serum and DSS derived from the control Nottingham cohort.
128 This primer site is also situated within the RT domain of the polymerase gene, allowing for
129 genotyping and determination of some RAS. A second widely used primer set (F2, F3, R2 and
130 R3; (10)) was subsequently tested to generate larger amplicons and thus greater DNA
131 sequence information. The sets were further tested in a variety of combinations to generate
132 amplicons of intermediate length overlapping in genomic coverage.

133 **Sanger sequencing and phylogeny:** PCR-positive products were diluted 1:10 with water and
134 couriered at ambient temperature for sequencing by a commercial service (Source

135 Bioscience, Nottingham, UK). Short products were sequenced with F1 primer only, and
136 longer F1/R3 and F3/R1 products were sequenced with both F1 and R1 primers. These reads
137 were assembled to produce a complete contiguous sequence covering PreS2/S. Sequences
138 used for phylogenetic analysis were aligned using MUSCLE in MEGA X (11, 12), and
139 maximum likelihood trees constructed using a General Time Reversible model in MEGA X.
140 Samples containing deletions were excluded from the tree. Sequences were deposited in
141 GenBank under accession numbers MK517481 – MK517524.

142 **MinION sequencing library preparation:** Three high titre (>10^7 IU/mL) samples from both
143 Brazil and Iraq cohorts were selected for sequence analysis. Barcoded samples were
144 prepared for MinION sequencing using a two stage PCR approach and the SQK-LWB001
145 library preparation kit. First round PCR was carried out as above, using 25 µL Hemo KlenTaq
146 reactions with 3 mm^2 punches from DSS. F4 and R4 primers were used as specified in table
147 1. From this reaction, 1 µL of product was then used as the template for a 50 µl PCR
148 containing 25 µL 2x LongAmp HotStart Taq master mix, 1.5 µL of barcoded primer mix
149 (supplied by ONT) and 22.5 µL nuclease free water. Products were then prepared according
150 to the SQK-LWB001 kit protocol. Briefly, PCR products were bound to AMPure XP beads
151 (Beckman Coulter) and washed with 70 % ethanol, before eluting in 10 µL 10mM Tris-HCl
152 (pH 8.0) with 50mM NaCl. Cleaned products were then quantified by Qubit using the dsDNA
153 high sensitivity kit (Thermo Fisher). Based on the method developed by Quick *et al*. (7),
154 amplicons were pooled to achieve a total of 0.3 pM input DNA per MinION flow cell,
155 therefore for 1.3 kb amplicons this equates to ~260 ng total DNA. Following ligation of rapid
156 sequencing adapters, the library was run for 48hrs on a MinION Mk II through a computer
157 running MinKNOW 1.10.16 in Microsoft Windows followed by basecalling using Albacore

158 2.2.2. Adapter-trimmed sequences were uploaded to the NCBI Sequence Read Archive
159 under project ID PRJNA521740.

160 **MinION sequencing analysis:** Basecalled reads were trimmed using Porechop 0.2.3 using
161 high stringency settings (--discard_middle and --require_two_barcodes) and retained when
162 Porechop and Albacore barcode aligners were in agreement. NanoPlot was used to inspect
163 read quality and length, and reads were filtered based on length using NanoFilt (13) to a
164 minimum length of 1200 and maximum length of 1300 nucleotides.

165 Processed reads were used as the input for Canu (v1.7.1) (14), a *de novo* genome assembler
166 optimised for use with long, error-prone reads. The same reads were subsequently aligned
167 using Minimap2 (15) to their respective consensus sequences generated by Canu and
168 manually inspected using IGV (Broad Institute) to ensure complete coverage and to inspect
169 for significant structural variants. Alignments were further processed using Nanopolish
170 v0.10.2 (8), using the Variants module and the --fix-homopolymers function to generate a
171 corrected consensus sequence. A full description of the bioinformatics workflow used is
172 included as supplementary data. As validation Sanger sequences were produced by
173 sequencing amplicons with both F1 and R1 primers, these were used as the “gold standard”.
174 Canu and Nanopolish consensus sequences were aligned with their respective Sanger contig
175 using MEGA.

176 **Genotyping and variant calling:** For both Sanger and MinION sequence data genotypes
177 were determined using the web-based tool HBV geno2pheno (16). Known HBV treatment
178 resistance and immune escape variants were screened using the hepatitis B virus database
179 (HBVdb (17)). Mutations against the genotype consensus reference sequences used in
180 geno2pheno that were not flagged as clinically significant are provided in supplementary

table 1. For samples sequenced by MinION potential intra-host variants were screened for by aligning sequencing reads to the corresponding nanopolished consensus sequence for each sample and using the *variants* module within Nanopolish, with 0.1 set as the minimum frequency required to call a SNP.

Results

Primer analysis for PCR amplification of HBV from DSS.

Initially we assessed three previously described primer sets for amplification of regions of the HBV genome using Hemo KlenTaq polymerase. A known HBV-positive serum sample with viral load >10^7 IU/mL was diluted 10-fold and spotted onto DSS cards. Using direct PCR of punched-out discs from these cards, HBV amplicons were obtained using all the primer pairs analysed (table 2). Amplification of the smallest product, using primers F1 and R1, was the most sensitive approach, amplifying a product from a sample containing as little as 1 x 10^3 IU/mL. Larger products (over 700 bp) were achieved using these primers in combination with the F3 and R3 primers down to 10^4 IU/mL. Subsequent investigation demonstrated that PCR amplification using Phusion Blood Direct polymerase allowed for increased sensitivity when amplifying small products, down to 600 IU/mL but gave little improvement in sensitivity when amplifying larger products (data not shown).

Sanger sequencing direct from DSS

Following this assessment, primer pairs F1/R1, F1/R3 and F3/R1 (figure 1) were used with Phusion Blood Direct polymerase for the analysis of 30 HBV-positive serum samples of defined viral load isolated in Brazil (table 3). Limited treatment information was available for some of the samples. Amplicons were achieved for all but 3 samples using the F1/R1 primer pair. The amplicon generated by this primer pair (281 bp) was sufficient to enable virus genotyping and limited detection of escape mutants by conventional Sanger sequencing. The 27 successfully genotyped samples divided into subtypes as follows: seven A1, two A2, one B1, two D1, two D1, two D2, nine D3, one F1 and three F2 (table 3).

It was not clear why three of the samples could not be amplified using the F1/R1 primer pair, but it is likely due in part to lower viral load as all three had viral loads of ~1 x 10^3 – 1 x 10^4 IU/mL (table 3). As the genotypes of these samples had not been previously determined it was not possible to confirm whether the primer pair had a lower sensitivity for some genotypes.

Successful amplification of the larger products using primer pairs F1/R3 and F3/R1 appeared to be associated with viral load (table 3). Both primer pairs were able to generate amplicons from samples of viral load >10^6 IU/mL. F3/R1 displayed a higher sensitivity for genotype D samples as amplicons were achieved for samples Br13 and Br16 (viral loads 5.99 x10^5 and 2.58 x10^5 IU/mL, respectively), although no amplicon was obtained for the higher viral load sample Br12 (9.41 x 10^5 IU/mL).

Genotyping and RAS characterisation

The amplicon produced from the F1/R3 primers permitted Sanger sequencing across aa 169 to aa 250 of the reverse transcriptase (RT) domain of the Pol gene (figure 1, highlighted in red), allowing identification of resistance associated substitutions (RAS). A restricted section of this crucial RT RAS region can be sequenced with the amplicons produced from the other two primer pairs. Of those samples for which an amplicon was obtained, two samples contained known polymerase RAS. The dominant sequence amplified for Br3 contained V173L, L180M and M204V, which in isolation or combination confer resistance to lamivudine, entecavir and telbivudine. The predominant sequence in sample Br9 only contained the V173L mutation which, in isolation, is not associated directly with resistance to any of the clinically approved polymerase inhibitors.

Having refined the workflow for HBV genotyping and RAS-typing by Sanger sequencing from DSS of samples with known viral load, we applied it to a second sample set to assess the broader application of the workflow. Seventy serum samples isolated from HBV-positive patients in the Kurdistan Region of Iraq were processed onto DSS cards and shipped to the UK for analysis. Amplicons were obtained for 11 of the 70 samples and Sanger sequencing revealed they were all genotype D (table 4). Although successful amplification correlated with higher viral load (figure 2), the sensitivity of the amplification PCR for these samples was markedly lower compared to the Brazilian cohort. It is not clear why it was possible to generate amplicons for two Iraqi DSS samples of comparatively low viral load (1.15×10^4 and 2.58×10^2 IU/mL), or why three high viral load samples could not be amplified (2.28×10^8, 1.60×10^7 and 1.42×10^7 IU/mL).

While no RT RAS were detected, three samples contained known sAg immune escape mutants, demonstrating that this process can provide clinically relevant sequence information from poorly characterised samples.

Samples from both cohorts demonstrated clustering by genotype when plotted on a maximum likelihood tree with respective genotype references from GenBank (figure 3).

MinION sequencing direct from DSS

Having obtained clinically relevant sequence data by Sanger sequencing from DSS, we investigated whether comparable data could be obtained using MinION sequencing. Three samples each were selected from the Brazilian and Iraqi cohorts (Br1, Br2 and Br3; Iq2, Iq3 and Iq4), that had been successfully amplified with all three primer pairs. Amplicons of 1,274 bp were generated using primers F4 and R4, which were analysed in parallel by Nanopore sequencing. A total of 185,349 raw reads were obtained for the 6 samples,

ranging from 23869 to 41392 per barcode. Following adapter trimming and further filtering of erroneously long and short reads these counts ranged from 7676 to 11832 per barcode (table 5). A summary of raw sequencing reads acquired over time, and average quality score per read over time is included in figure 4.

Accurate consensus sequences generated by MinION Nanopore sequencing

Consensus sequences were assembled using Canu. Following assembly, the only errors observed were single base deletions within homopolymers. These ranged from 5 to 12 deletions within the total amplicon (table 6). Following a single round of Nanopolish all sequences were identical to their Sanger counterparts. Workflows for the two sequencing procedures are shown in figure 5. Upon receipt of samples it is feasible to obtain accurate sequences either by Sanger or MinION within 1-2 days.

Detection of minor variants with minION

A number of putative minor variants were detected by aligning minION reads with the consensus sequence, the majority of which were filtered out by Nanopolish. Of the remaining variants samples Br1, Br2, Iq1, Iq3 and Iq4 contained sequences with the P217L polymorphism in sAg in around 18% of reads, which is associated with immune escape. Iq3 also contained a L109P mutant in sAg in 16% of sequencing reads, associated with increased hydrophobicity. However, comparison with Sanger sequencing showed that neither of these base changes were visible as minor peaks on the electropherogram of the corresponding samples.

279

280

281

282

283

284

285

286

Discussion

HBV has the capacity to exist in a host as a population of closely related viruses (18). While not displaying the extreme variability associated with RNA viruses, error-prone reverse transcription facilitates rapid adaptation to the host environment. As a consequence, resistance to antiviral therapies is common. Methods to both genotype and characterise RAS in parts of the world without access to conventional laboratory and sequencing facilities would be clinically beneficial. These techniques may become increasingly important in places such as sub-Saharan Africa, where antiretroviral programmes are in place for HIV treatment but HBV prevalence and development of resistance to drugs such as lamivudine is not accounted for (19, 20). As HIV mortality decreases and life expectancy increases, the development of chronic liver disease due to HBV infection will be of increasing concern.

We have demonstrated that clinically useful HBV sequence data can be obtained from DSS, with a lower-limit of detection of approximately 600 IU/mL, using a relatively cost-effective method that requires no cold chain. Several of the RAS detected in this cohort are clinically significant. The Y100C mutant in the S region of HBsAg has been linked to false negative/low HBsAg tests (21), and appears to be common in our Brazilian cohort, being present in 5/10 genotype A samples. More significantly, as it targets the RT domain of Pol, this method allows characterisation of drug resistance markers, which is potentially valuable in countries where prescription of drugs known to select for HBV resistance is common. The V173L, L180M and M204V RAS detected in the polymerase gene indicate resistance to the nucleoside analogues lamivudine and entecavir.

Although our original methodology removed the need for a cold chain and required only basic or mobile laboratory facilities, a Sanger sequencer (or access to a sequencer-equipped

311 laboratory to where DSS/amplicons can be shipped) was still required. We therefore aimed
312 to combine our DSS method with nanopore sequencing, increasing portability and to
313 provide a method that can be rapidly deployed in resource-poor settings.

314 NGS datasets were successfully generated for all of the six of the samples tested. All
315 samples demonstrated the characteristic error profile associated with nanopore
316 sequencing, with frequent indels in homopolymers of 3 bases or more (22). In all cases
317 these miscalls were removed using Nanopolish. These errors, which occur when voltage
318 signal remains constant across homopolymer templates passing through the nanopore, will
319 potentially become less of an issue with improved software interpolation or the
320 development of new protein nanopores. In all cases the data was sufficiently accurate that
321 the assembly generated by Canu, including indels, could be used to reliably and quickly
322 genotype without any further processing, and with subsequent processing in Nanopolish
323 produced sequences that were 100% identical to the sequence reads generated by Sanger
324 sequencing. This method is therefore of use in situations where Sanger sequencing is
325 unavailable and illustrates the utility of the MinION as a portable sequencer to determine
326 the consensus of a virus population.

327 Sanger sequencing of HBV enables characterisation of a consensus sequence of theoretically
328 the most abundant nucleotide at each position in a viral sequence within a sample.
329 Inspection of minor peaks on the electropherogram allows detection of minor sequence
330 variants, down to a prevalence of around 20%, dependent on sample quality. As has been
331 previously shown with HBV, next generation sequencing approaches allow characterisation
332 of minor variants at a lower threshold (23-25). This information is potentially clinically
333 useful, enabling earlier detection of resistant viruses, informing selection of appropriate

334 treatment regimens. Accurately determining these minor variants with NGS is
335 methodologically difficult, as low concentrations of viral template often necessitate the use
336 of PCR before sequencing. This may introduce bias from a range of sources. A recent
337 investigation (26) suggested that if PCR primers are well designed an amplicon sequencing
338 approach can be as reliable as unbiased metagenomic sequencing. However, the authors
339 highlighted that in its current level of development, MinION sequencing is not appropriate
340 for discovering novel, low-level intra-host sequence variants due to the high false-discovery
341 rate. In our data, we applied a conservative variant calling approach by aligning all sequence
342 reads to the consensus followed by variant calling using Nanopolish.

343 Sequencing HIV from dried blood spots using 454 pyrosequencing previously showed almost
344 complete concordance with Sanger (27), but discrepancies appeared when characterising
345 minor variants, particularly in low titre samples (28). Further experiments using more
346 appropriate variant calling workflows, and a side-by-side comparison of DSS, direct serum
347 and DNA extract would be required to study the potential effect of storing DSS samples on
348 measures of diversity. The majority of candidate variants in our data were filtered out using
349 Nanopolish, suggesting they could be false-positives caused by sequencer error. A variant
350 that remained unfiltered was present in 5 of 6 samples (and therefore was not genotype
351 specific), the mutation, P217L in S has previously been linked to diagnostic escape (29). The
352 other minor variant, L109P in S, was present in a single sample (Iq1), and has been linked to
353 an increase in hydrophobicity (30), but the significance of this phenotype has not been
354 determined.

355 The MinION sequencing protocol described here followed the manufacturer's
356 recommended protocol, using the standard 48-hour script in order to maximise read depth.

As demonstrated elsewhere (31), an alternative approach is to run the MinION for a shorter amount of time, flush the flow cell and add different samples. Larger barcode kits (up to 96) and custom barcodes can also be used. With this assay, setup can be adjusted to favour either assay throughput or read depth, prioritizing rapid consensus sequence generation or interrogation of intra-sample diversity. The metrics produced by the sequencer as shown in figure 4 can aid in this optimisation and be used to determine the optimum timepoint to stop a sequencing run and add more samples, in order to ensure efficient use of resources. Based on current prices, and after an initial outlay on basic lab equipment (PCR machine, pipettes), we estimate that accurate sequence data with the MinION could be obtained for as little as 20 GBP per sample. In comparison, a single Sanger read across the region studied in this paper will cost ~4 GBP, with larger regions requiring at least 2 reads for complete coverage.

One limitation of this method is the amount of template input required for successful amplification; obtaining long amplicons (in this case ~1247 bp) suitable for MinION sequencing required serum spots generated from samples with viral titre of at least 10^6-10^7 IU/mL. As expected, successful amplification was inversely correlated with viral load, making assays which involve amplifying all or most of S in a single amplicon only applicable to high titre samples. The combination of F4/R4 primers was chosen to take advantage of the long reads available with MinION sequencing. Increased sensitivity could be achieved using a PCR-tiling approach of two or more amplicons that are pooled before sequencing (as demonstrated with the much larger Zika genome (7)), or by scaling up reaction mixtures and using more DSS per reaction.

The workflow described in figure 6 is intended as a starting point for a diagnostic workflow, but, as indicated above, this method can be modified at each point to address specific clinical questions with different pathogens. In our application, dried serum spots were studied based on available samples, but the modified *Taq* enzymes used are suitable for use with whole blood, plasma or serum added directly to the PCR reaction. There is also the potential to apply this approach to other viruses where high-throughput testing is desired, for example improving existing workflows for cytomegalovirus (32).

In summary, we describe two approaches for rapid genotyping and RAS detection in hepatitis B virus, which are applicable in resource-limited settings and require little existing infrastructure. The results presented here demonstrate the utility of direct PCR enzymes and DSS together in a clinical context. To our knowledge this has not been previously described. We have also demonstrated, for the first time, that nanopore sequencing can be applied directly to samples amplified from serum spots. Reliable sequence data was generated using the MinION sequencer, removing the need for reliance on laboratory infrastructure. Although accurate consensus sequences can be generated, it is likely that both the software and hardware associated with nanopore sequencing will require improvement before this method will find routine use for detecting minor variants within a virus population.

Funding

Funding was provided by the Nottingham Molecular Pathology Node (MRC/EPSRC grant MR/N005953/1) and the National Institute for Health Research (NIHR) Nottingham Biomedical Research Centre.

Author contributions

CPM, AWT, WLI and SA designed the experiments; MMCNS, ACGJ, JFS, PJ, CHS and FTS provided samples and associated clinical data and prepared DSS cards; SA, EP and CPM carried out the experimental work; SA carried out nanopore sequencing and associated bioinformatics; SA, BK, AWT and CPM analysed the data and drafted the manuscript; all authors edited the manuscript.

Tables

Primer name	This study	Sequence (5'-3')	HBV genome position*
Outer plus [9]	F1	GATGTGTCTGCGGCGTTTTA	376 - 395
Outer minus [9]	R1	CTGAGGCCCACTCCCATAGG	656-637
HBVP [10]	F2	TCATCCTCAGGCCATGCAGT	3198-3217
HBVM [10]	R2	GACACATTTCCAATCAATNGG	989-970
HBVZ [10]	F3	AGCCCTCAGGCTCAGGGCATA	3085-3105
HBV3 [10]	R3	CGTTGCCKDGCAACSGGGTAAAGG	1163-1140
HBVZ-ONT	F4	TTTCTGTTGGTGCTGATATTGCAGCCCTCAGGCTCAGGGCATA	3085-3105
HBV3-ONT	R4	ACTTGCCTGTCGCTCTATCTTCCGTTGCCKDGCAACSGGGTAAAGG	1163-1140

Table 1: Primers used for the amplification of HBV. F4 and R4 primers contain 22 bp sequences at the 5' end for MinION library preparation PCR. *Numbering based upon HBVdb genotype A master strain X02763 (17).

	Primer pair					
IU/mL HBV	**F1+R1 (281 bp)**	**F2+R2 (1,013 bp)**	**F1+R2 (614 bp)**	**F2+R1 (680 bp)**	**F1+R3 (788 bp)**	**F3+R1 (793 bp)**
1.2×10^7	+	+	+	+	+	+
1.2×10^6	+	+	+	+	+	+
1.2×10^5	+	+	+	+	+	+
1.2×10^4	+		+	+	+	+
1.2×10^3	+				+	+
1.2×10^2						
1.2×10^1						

428

429 **Table 2: HBV amplification success using different primer combinations.** HBV amplicon

430 sizes at different viral loads from DSS using a serially diluted high-titre HBV-positive sample.

431 Predicted amplicon size (in base pairs) is noted below primer pairing in brackets. +, indicates

432 successful amplification or single discrete band following analysis by agarose gel

433 electrophoresis.

434

Sample	Viral load (IU/mL)	Therapy	F1+R1 product	Genotype	F1+R3 product	RT domain RAS	F3+R1 product	sAg escape mutants
Br1	816,483,772	No treatment	Y	A1	Y	-	Y	Y100C
Br2	389,547,123	Peg-IFN	Y	A1	Y	-	Y	Y100C
Br3	241,145,063	TDF, 3TC	Y	D2	Y	V173L, L180M M204V	Y	-
Br4	33,875,365	TDF, 3TC, EFV	Y	A1	Y	-	Y	Y100C
Br5	21,807,740	No treatment	Y	D3			Y	-
Br6	6,219,005	TDF	Y	D3	Y	-	Y	-
Br7	5,843,310	No treatment	Y	A1	Y	-	Y	Y100C
Br8	5,217,998	nd	Y	D3	Y	-	Y	-
Br9	3,166,098	TDF	Y	F2	Y	V173L		-
Br10	692,965	nd	Y	A2				
Br11	193,271	TDF	Y	F2				
Br12	94,152	nd	Y	D3				
Br13	59,927	TDF	Y	D3			Y	
Br14	43,005	TDF, 3TC	Y	A1				Y100C
Br15	35,672	TDF	Y	A1				
Br16	25,791	TDF	Y	D2			Y	
Br17	17,280	nd	Y	F1				
Br18	16,697	nd	Y	D3				
Br19	12,446	3TC	Y	D3				
Br20	12,196	No treatment	Y	D1				
Br21	10,058	TDF	Y	F2				
Br22	7,199	TDF		ng				
Br23	6,208	No treatment	Y	D3				
Br24	4,091	TDF	Y	B1				
Br25	2,884	Peg-IFN	Y	A1				
Br26	2,431	No treatment	Y	D1				
Br27	2,262	No treatment	Y	A2				
Br28	1,069	nd		ng				
Br29	1,046	No treatment		ng				
Br30	635	No treatment	Y	D3				

Table 3: Amplification of S/Pol gene from DSS of HBV-positive samples from Brazil, allowing genotyping and characterisation of RAS, is dependent on viral load. Clinically significant RAS in the reverse transcriptase (RT) domain of the Polymerase open reading frame (ORF) are noted. TDF, tenofovir; 3TC, lamivudine; EFV, efavirenz; nd, no treatment data available; ng, not genotyped. Blank fields for primer pair products indicate no amplicon was generated.

441
442

Sample	Viral load (IU/mL)	F1+R1 product	Genotype	F1+R3 product	RT domain RAS	F3+R1 product	sAg escape mutants
Iq1	745,867,080	Y	D1	Y	-	Y	-
Iq2	480,199,200	Y	D1	Y	-	Y	-
Iq3	369,094,710	Y	D1	Y	-	Y	-
Iq4	361,383,300	Y	D1	Y	-	Y	-
Iq5	330,190,500	Y	D1	Y	-	Y	-
Iq6	17,996,700	Y	D1	Y	-		P120S
Iq7	12,637,111	Y	D1	Y	-	Y	P120S
Iq8	3,393,900	Y	D3	Y	-		
Iq9	1,843,350	Y	D1	Y	-		G145R
Iq10	11,514	Y	D1	Y	-		Q101H, Y143H
Iq11	258	Y	D1	Y	-		

443 **Table 4. Amplification of S/Pol gene from DSS of HBV-positive samples in Iraq cohort.**

444 Amplicons were generated from 11 of 71 DSS samples collected in the Kurdistan Region of
445 Iraq. Clinically significant RAS in the reverse transcriptase (RT) domain of the Polymerase
446 open reading frame (ORF) are noted.

447

Sample	Raw reads	Adapter trimming	Length filtered
Br1	24105	13320	11272
Br2	23868	12640	10309
Br3	41392	14702	11832
Iq2	27860	11654	9572
Iq3	27478	12445	7676
Iq4	40646	13539	8979

448 **Table 5. MinION sequencing yields**. Raw reads are those assigned barcodes by Albacore
449 before any further quality control. Adapter trimmed reads are those exceeding a mean
450 Phred score of 7 and processed by Porechop. Length filtered reads were processed by
451 NanoFilt.

452

453

Sample	Mismatches between Canu assembly and Sanger	Mismatches between Nanopolish consensus and Sanger
Br1	5	0
Br2	6	0
Br3	5	0
Iq2	9	0
Iq3	12	0
Iq4	6	0

454 **Table 6:** Agreement between minION sequenced samples and Sanger across the 1,274bp

455 region studied.

456
457
458

Supplementary data

Bioinformatics workflow

Following basecalling using Albacore, the "pass" folder (reads exceeding a mean Phred score of 7) was used as the input for Porechop as follows:

porechop -i source_directory --discard_middle --require_two_barcodes

Filtering based on length was carried out in NanoFilt:

cat reads.fastq | nanofilt -l 1200 --maxlength 1300 > reads.filtered.fastq

Downsampled, filtered FASTQ files for each sample were then used as the input for Canu:

./canu --nanopore-raw reads.filtered.fastq genomeSize=1300 stopOnReadQuality=false -d canu_out -p sample-ID

This generates several candidate contigs, the contig with the highest number of reads used was verified using BLAST and taken forwards to the next step.

Reads were then aligned in Minimap2 to their respective contig generated using Canu:

minimap2 -ax map-ont canu_contig.fasta reads.filtered.fastq | samtools view -bS - | samtools sort -o sample.minimap.sorted.bam

This alignment was then used to generate a polished consensus sequence using Nanopolish. First the reads are indexed to match every read in the .fastq file with its corresponding raw fast5 file (the original output of the minION sequencer):

nanopolish index -d fast5_directory -s sequencing_summary.txt reads.filtered.fastq

The alignment, reference contig and fastq for each sample were then used as the input for Nanopolish:

nanopolish variants --consensus --fix-homopolymers -b sample.minimap.sorted.bam -g canu_contig.fasta -r reads.filtered.fastq -o sample.polished.consensus.vcf

This consensus .vcf file was then converted to standard .fasta format:

nanopolish vcf2fasta -g canu_contig.fasta sample.polished.consensus.vcf > sample.polished.consensus.fasta

The output consensus sequence can then be checked against the original Canu contig, as well as a Sanger contig from the same sample if available. These sequences can also be used for genotyping and resistance typing against established reference sequences.

Intra-sample variants can be determined by aligning all reads to the Nanopolished consensus sequence or Sanger contig and using the *variants* function within Nanopolish to generate a .vcf file:

nanopolish variants -b alignment.sorted.bam -g consensus.fasta -r sample.fastq -o variants.vcf --min-candidate-frequency 0.1 --ploidy 1

ID	Genotype	sAg mutants	Pol mutants
Br1	A1	Y100C, S207N	D7N, N122H, M129L, W153R, V163I, I253V, V278I, M336L, V341P
Br2	A1	Y100C, S207N	D7N, N122H, M129L, W153R, V163I, I253V, V278I, M336L
Br3	D2	T118A, E164D, I195M	Y45H, H126R, V173L, H126R, V173L, L180M, M204V, K270R
Br4	A1	G44E, Y100C, S207N	N122H, M129L, W153R, V163I, I253V, V278I, M336L
Br5	D3	T127P	F122L, Q130P, Y135S
Br6	D3	T127P	F122L, Q130P, Y135S, S176R
Br7	A1	Y100C	S117P, N122H, M129L, W153R, V163I
Br8	D3	I110L, G112N, S114P, T125M	N118T, R120K, I121F, F122A, N123D, Q130P, Y135N, S176R
Br9	F2		N123D, M129L, S137T, V173L
Br10	A2		D7A, I53V
Br11	F2		N123D, M129L, S137T, S176R
Br12	D3	T127P, Y134N	F122L, H124N, Q130P, Y135S, V142E, S176R
Br13	D3	T127P	F122L, Q130P, Y135S
Br14	A1	Y100C	N122H, N123D, M129L, W153R, V163I
Br15	A1	Y100C	N122H, M129L, W153R, V163I, S176R
Br16	D2	T118A, R122K, T127P, A128V, G159A, F161I	N118D, H126R, Y135S, Q149K, K168E, I169N, S176R
Br17	F1	S140T	N123D, M129L, S173T, F148Y, L151F
Br18	D3	T127P	F122L, Q130P, Y135S
Br19	D3	T127P	F122L, Q130P, Y135S
Br20	D1		
Br21	F2	S140T	N123D, M129L, S173T, F148Y, S176R
Br22	ng		
Br23	D3	T127P	F122L, Q130P, Y135S, S176R
Br24	B1		N124D, N131D, S176R
Br25	A1	Y100C	N122H, Y126H, M129L, W153R, V163I
Br26	D1	F93L, T127P	L102I, V112A, Y135S, S176R
Br27	A2	T114S	N122I, D134N, W153R, S176R
Br28	ng		
Br29	ng		
Br30	D3	G119A, C124S, T127P, Q129E, Y143N, P135T, G145E, T148S, I152L, P153T	L115V, F122L, T128S, Q130P, L132Q, D134H, Y135S, S137*, V142E, S143Y, H156Q, H160S, P161H, S176R
Iq1	D1	T127P	S109P, Y135S
Iq2	D1	T127P	Y135S
Iq3	D1	T127P	Y135S
Iq4	D1	T127P	Y135S
Iq5	D1	T127P	M129L, Y135S, S176R
Iq6	D1	Q101H, P120S, T127P	T128I, M129L, Y135S, S176R
Iq7	D1	P120S, T127P	T128I, Y135S, S176R
Iq8	D3	T127P	Y135S
Iq9	D1	S114A, T125M, G145R	F122R, H124N, Q130P, N131D, R153Q, S176R
Iq10	D1	Q101H, T127P, Y134H, T140I	M129L, Y135S, V142A, S176R
Iq11	D1	T127P	Y135S, S176R

Supplementary table 1: Mutations vs consensus reference sequences determined from Sanger sequencing in geno2pheno.

References

1. WHO. 18 July 2018 2018. Hepatitis B virus Fact sheet, *on* World Health Organisation. http://www.who.int/en/news-room/fact-sheets/detail/hepatitis-b. Accessed
2. Graber-Stiehl I. 2018. The silent epidemic killing more people than HIV, malaria or TB. Nature 564:24.
3. Lemoine M, Eholie S, Lacombe K. 2015. Reducing the neglected burden of viral hepatitis in Africa: strategies for a global approach. J Hepatol 62:469-76.
4. Lazarevic I. 2014. Clinical implications of hepatitis B virus mutations: recent advances. World J Gastroenterol 20:7653-64.
5. Lapinski TW, Pogorzelska J, Flisiak R. 2012. HBV mutations and their clinical significance. Adv Med Sci 57:18-22.
6. Quick J, Loman NJ, Duraffour S, Simpson JT, Severi E, Cowley L, Bore JA, Koundouno R, Dudas G, Mikhail A, Ouedraogo N, Afrough B, Bah A, Baum JH, Becker-Ziaja B, Boettcher JP, Cabeza-Cabrerizo M, Camino-Sanchez A, Carter LL, Doerrbecker J, Enkirch T, Dorival IGG, Hetzelt N, Hinzmann J, Holm T, Kafetzopoulou LE, Koropogui M, Kosgey A, Kuisma E, Logue CH, Mazzarelli A, Meisel S, Mertens M, Michel J, Ngabo D, Nitzsche K, Pallash E, Patrono LV, Portmann J, Repits JG, Rickett NY, Sachse A, Singethan K, Vitoriano I, Yemanaberhan RL, Zekeng EG, Trina R, Bello A, Sall AA, Faye O, et al. 2016. Real-time, portable genome sequencing for Ebola surveillance. Nature 530:228-232.
7. Quick J, Grubaugh ND, Pullan ST, Claro IM, Smith AD, Gangavarapu K, Oliveira G, Robles-Sikisaka R, Rogers TF, Beutler NA, Burton DR, Lewis-Ximenez LL, de Jesus JG, Giovanetti M, Hill SC, Black A, Bedford T, Carroll MW, Nunes M, Alcantara LC, Jr., Sabino EC, Baylis SA, Faria NR, Loose M, Simpson JT, Pybus OG, Andersen KG, Loman NJ. 2017. Multiplex PCR method for MinION and Illumina sequencing of Zika and other virus genomes directly from clinical samples. Nat Protoc 12:1261-1276.
8. Loman NJ, Quick J, Simpson JT. 2015. A complete bacterial genome assembled de novo using only nanopore sequencing data. Nat Methods 12:733-5.
9. Brechtbuehl K, Whalley SA, Dusheiko GM, Saunders NA. 2001. A rapid real-time quantitative polymerase chain reaction for hepatitis B virus. J Virol Methods 93:105-13.
10. PHE. 2007. Hepatitis B (HBV): Genotyping protocol, *on* Public Health England. https://www.gov.uk/government/publications/hepatitis-b-hbv-genotyping-protocol. Accessed 30 Oct 2007.
11. Kumar S, Stecher G, Li M, Knyaz C, Tamura K. 2018. MEGA X: Molecular Evolutionary Genetics Analysis across Computing Platforms. Mol Biol Evol 35:1547-1549.
12. Edgar RC. 2004. MUSCLE: multiple sequence alignment with high accuracy and high throughput. Nucleic Acids Research 32:1792-1797.
13. De Coster W, D'Hert S, Schultz DT, Cruts M, Van Broeckhoven C. 2018. NanoPack: visualizing and processing long-read sequencing data. Bioinformatics 34:2666-2669.
14. Koren S, Walenz BP, Berlin K, Miller JR, Bergman NH, Phillippy AM. 2017. Canu: scalable and accurate long-read assembly via adaptive k-mer weighting and repeat separation. Genome Res 27:722-736.
15. Li H. Minimap2: pairwise alignment for nucleotide sequences. Bioinformatics doi:10.1093/bioinformatics/bty191.

16. Beggel B, Neumann-Fraune M, Doring M, Lawyer G, Kaiser R, Verheyen J, Lengauer T. 2012. Genotyping hepatitis B virus dual infections using population-based sequence data. J Gen Virol 93:1899-907.
17. Hayer J, Jadeau F, Deléage G, Kay A, Zoulim F, Combet C. 2013. HBVdb: a knowledge database for Hepatitis B Virus. Nucleic Acids Research 41:D566-D570.
18. McNaughton AL, D'Arienzo V, Ansari MA, Lumley SF, Littlejohn M, Revill P, McKeating JA, Matthews PC. 2019. Insights From Deep Sequencing of the HBV Genome-Unique, Tiny, and Misunderstood. Gastroenterology 156:384-399.
19. Barth RE, Huijgen Q, Taljaard J, Hoepelman AI. 2010. Hepatitis B/C and HIV in sub-Saharan Africa: an association between highly prevalent infectious diseases. A systematic review and meta-analysis. Int J Infect Dis 14:e1024-31.
20. Matthews PC, Geretti AM, Goulder PJ, Klenerman P. 2014. Epidemiology and impact of HIV coinfection with hepatitis B and hepatitis C viruses in Sub-Saharan Africa. J Clin Virol 61:20-33.
21. Martin CM, Welge JA, Rouster SD, Shata MT, Sherman KE, Blackard JT. 2012. Mutations Associated with Occult Hepatitis B Virus Infection Result in Decreased Surface Antigen Expression In Vitro. J Viral Hepat 19:716-23.
22. Sárközy P, Molnár V, Fogl D, Szalai C, Antal P. 2017. Beyond Homopolymer Errors: a Systematic Investigation of Nanopore-based DNA Sequencing Characteristics Using HLA-DQA2. Periodica Polytechnica Electrical Engineering and Computer Science 61:231-237.
23. Cao L, Wu C, Shi H, Gong Z, Zhang E, Wang H, Zhao K, Liu S, Li S, Gao X, Wang Y, Pei R, Lu M, Chen X. 2014. Coexistence of hepatitis B virus quasispecies enhances viral replication and the ability to induce host antibody and cellular immune responses. J Virol 88:8656-66.
24. Liu F, Chen L, Yu DM, Deng L, Chen R, Jiang Y, Chen L, Huang SY, Yu JL, Gong QM, Zhang XX. 2011. Evolutionary patterns of hepatitis B virus quasispecies under different selective pressures: correlation with antiviral efficacy. Gut 60:1269-77.
25. Margeridon-Thermet S, Shulman NS, Ahmed A, Shahriar R, Liu T, Wang C, Holmes SP, Babrzadeh F, Gharizadeh B, Hanczaruk B, Simen BB, Egholm M, Shafer RW. 2009. Ultra-deep pyrosequencing of hepatitis B virus quasispecies from nucleoside and nucleotide reverse-transcriptase inhibitor (NRTI)-treated patients and NRTI-naive patients. The Journal of infectious diseases 199:1275-1285.
26. Grubaugh ND, Gangavarapu K, Quick J, Matteson NL, De Jesus JG, Main BJ, Tan AL, Paul LM, Brackney DE, Grewal S, Gurfield N, Van Rompay KKA, Isern S, Michael SF, Coffey LL, Loman NJ, Andersen KG. 2019. An amplicon-based sequencing framework for accurately measuring intrahost virus diversity using PrimalSeq and iVar. Genome Biol 20:8.
27. Ji H, Li Y, Graham M, Liang BB, Pilon R, Tyson S, Peters G, Tyler S, Merks H, Bertagnolio S, Soto-Ramirez L, Sandstrom P, Brooks J. 2011. Next-generation sequencing of dried blood spot specimens: a novel approach to HIV drug-resistance surveillance. Antivir Ther 16:871-8.
28. Ji H, Li Y, Liang B, Pilon R, MacPherson P, Bergeron M, Kim J, Graham M, Van Domselaar G, Sandstrom P, Brooks J. 2013. Pyrosequencing dried blood spots reveals differences in HIV drug resistance between treatment naive and experienced patients. PLoS One 8:e56170.

655 29. Weinberger KM, Bauer T, Bohm S, Jilg W. 2000. High genetic variability of the group-
656 specific a-determinant of hepatitis B virus surface antigen (HBsAg) and the
657 corresponding fragment of the viral polymerase in chronic virus carriers lacking
658 detectable HBsAg in serum. J Gen Virol 81:1165-74.
659 30. Baclig MO, Alvarez MR, Gopez-Cervantes J, Natividad FF. 2014. Unique surface gene
660 variants of hepatitis B virus isolated from patients in the Philippines. J Med Virol
661 86:209-16.
662 31. Mbala-Kingebeni P, Villabona-Arenas CJ, Vidal N, Likofata J, Nsio-Mbeta J, Makiala-
663 Mandanda S, Mukadi D, Mukadi P, Kumakamba C, Djokolo B, Ayouba A, Delaporte E,
664 Peeters M, Muyembe Tamfum JJ, Ahuka-Mundeke S. 2019. Rapid Confirmation of
665 the Zaire Ebola Virus in the Outbreak of the Equateur Province in the Democratic
666 Republic of Congo: Implications for Public Health Interventions. Clin Infect Dis
667 68:330-333.
668 32. Koontz D, Dollard S, Cordovado S. 2019. Evaluation of rapid and sensitive DNA
669 extraction methods for detection of cytomegalovirus in dried blood spots. Journal of
670 Virological Methods 265:117-120.
671
672

673 # Figures

674

675

676

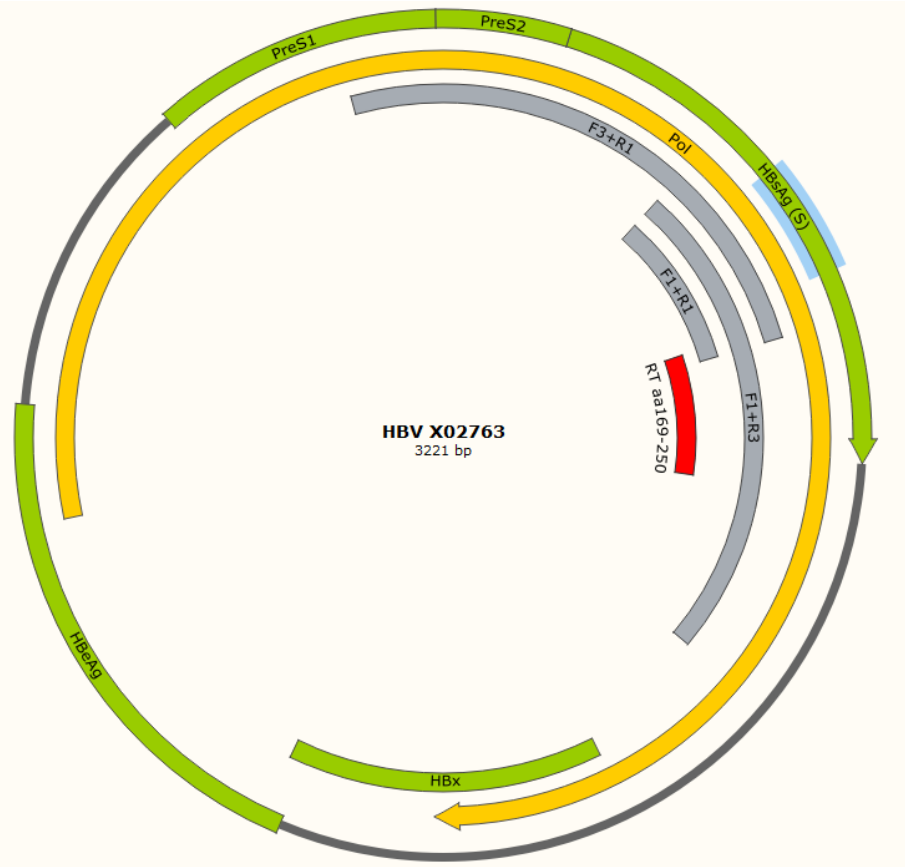

677

678 **Figure 1. Schematic of HBV PCR amplicons produced from cccDNA.** Regions covered by PCR

679 amplicons detailed in Table 2 are shown in grey. Overlapping ORFs in the HBV genome

680 (genotype A reference isolate X02763) are shown in green or yellow (polymerase gene).

681 Genome is represented as linear for clarity. F1+R1 amplicon is sufficient for genotyping and

682 limited detection of sAg escape mutants. The region of the reverse transcriptase domain

683 (RT) in which resistance associated substitutions (RAS) arise (aa169 – 250), shown in red, is

684 encompassed by the F1+R3 amplicon. The region in which known surface antigen (HBsAg)

685 immune/diagnostic escape mutants arise (aa100 – 147), highlighted in blue, is covered by all

686 three amplicons.

687

688

689

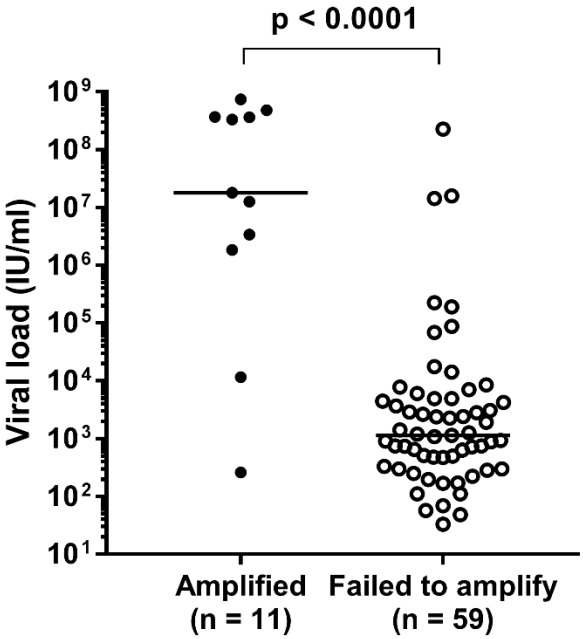

690

691 **Figure 2. HBV viral load of DSS from Iraq.** Successful PCR amplification of HBV-positive DSS

692 samples from Iraq is associated with higher viral load (Mann-Whitney U test). Number of

693 samples in each group (n) is shown. PCRs for samples which failed to amplify were

694 performed at least 3 times.

695

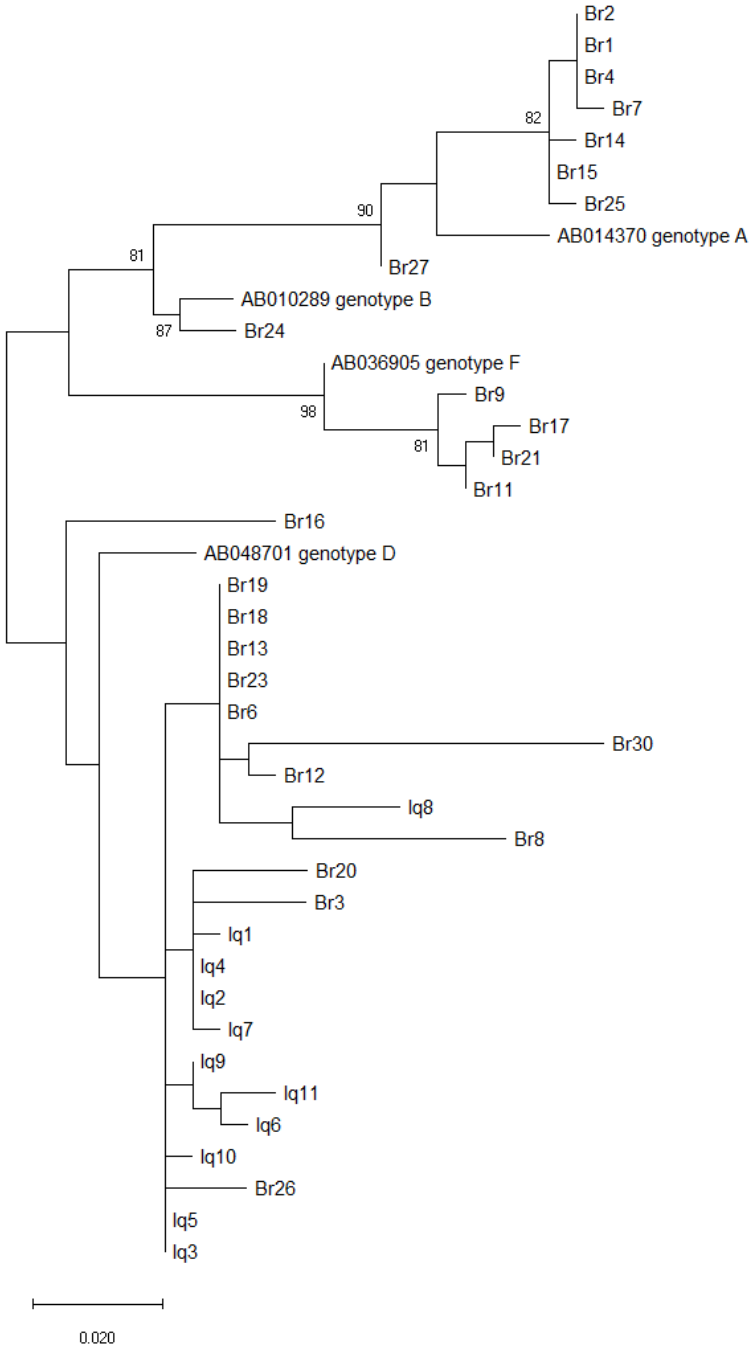

696

697 **Figure 3: Maximum likelihood (ML) tree constructed from F1+R1 PCR amplicon (240bp).**

698 The ML tree was inferred using a general time reversible model within MEGA X (11).

699 Statistical robustness was assessed using bootstrap resampling of 1,000 pseudoreplicates,

700 and the tree with the highest log-likelihood is shown.

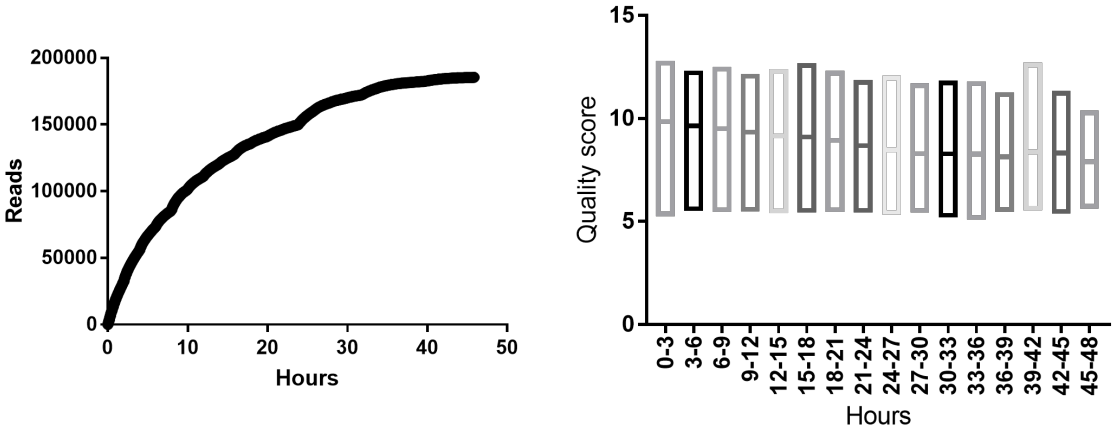

Figure 4. Metrics from MinION sequencing run. Both plots were generated from raw reads assigned barcodes by Albacore without further filtering. Quality scores are standard Phred scores produced by Albacore during basecalling, data is presented as mean Phred score per read with min and max.

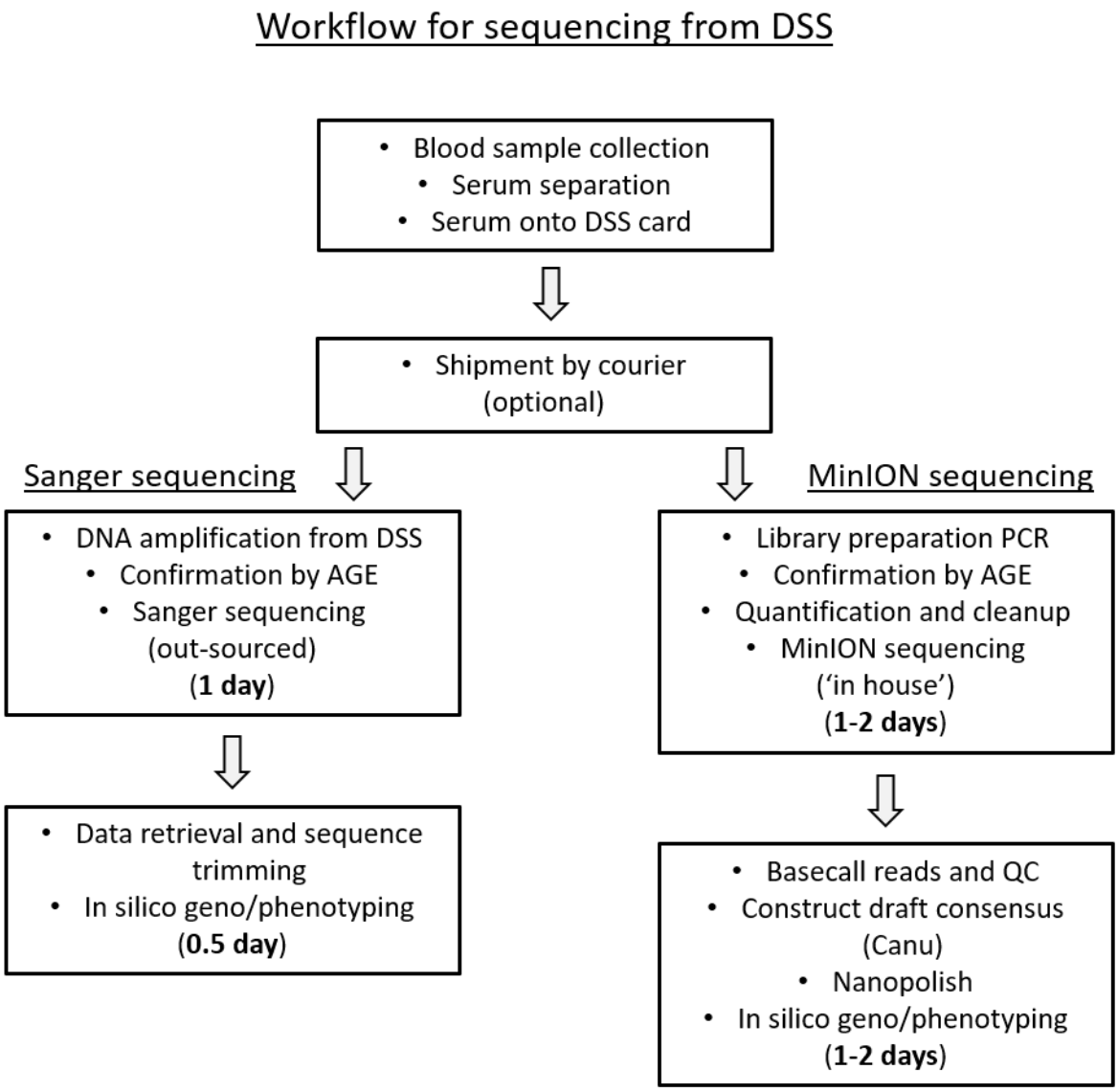

711

712 **Figure 5. Schematic of the sequencing workflows.** The typical number of days taken for
713 each aspect of the workflow is noted. The length of time given to the 'shipment by courier'
714 and Sanger sequencing steps are relevant to this study but may be omitted, or vary
715 significantly, depending upon the given laboratory and infrastructure situation. 1 day is
716 suggested as the minimum amount of time for MinION library preparation, sample clean up
717 and enough sequencing time to generate a reliable consensus. Sequencing to a greater
718 depth will add more sequencing and subsequent compute time. Sanger sequencing in
719 Nottingham is provided by a commercial service with sample collection and over-night

720 sequencing and data return. DSS, dried serum spot; AGE, agarose gel electrophoresis; QC,

721 quality control.

722

723